Electronic Supplementary Material (ESI) for Soft Matter.

Electronic Supplementary Information

Luminescent columnar discotics as highly efficient emitters in pure deep-blue OLEDs with an external quantum efficiency of 4.7%

Joydip De,[a] Ishan Sarkar,[a] Rohit Ashok Kumar Yadav,[b] Indu Bala,[a] Santosh Prasad Gupta,[c] Iram Siddiqui,[b] Jwo-Huei Jou,[b] and Santanu Kumar Pal*[a]

[a]*Department of Chemical Sciences, Indian Institute of Science Education and Research (IISER), Mohali, Punjab 140306, India*
[b]*Department of Materials Science and Engineering, National Tsing Hua University, Hsinchu 30013, Taiwan*
[c]*Department of Physics, Patna University, Patna-800005, India*

E-mail: skpal@iisermohali.ac.in, santanupal.20@gmail.com

Table of Contents **Page No.**

1) Materials and Methods

Materials. Chemicals and solvents (AR quality) were used as received without any further purification. Column chromatographic separations were performed on silica gel (100–200 & 230-400 mesh). Thin-layer chromatography (TLC) was performed on aluminium sheets pre-coated with silica gel (Merck, Kieselgel 60, F254).

Measurements and Characterization. *The instrumental details for structural characterization (NMR, HRMS, FT-IR), thermal characterization (polarized optical microscopy (POM), Thermogravimetric analysis (TGA), Differential scanning calorimetry (DSC), X-Ray diffraction (XRD)), photophysical studies (UV-Vis & Fluorescence), electrochemical (Cyclic voltammetry), electroluminescence (OLEDs) characterization are similar to as mentioned in our previous papers and reproduced below for the reader's convenience.*[1]

"Structural characterization of the compounds was carried out through a combination of infrared spectroscopy (IR) (Perkin Elmer Spectrum Two), ^{1}H NMR and ^{13}C NMR (Bruker Biospin Switzerland Avance-iii 400 MHz and 100 MHz spectrometers respectively), UV-vis-NIR spectrophotometers (Agilent Technologies, Cary 5000) and Mass spectrometry (Water Synapt G-2-s QTOF with MALDI ion source and α-cyano-4-hydroxy-cinnamic acid). IR spectra were recorded in neat form for target compounds. ^{1}H NMR spectra were recorded using deuterated dichloromethane (CD_2Cl_2) as solvent and tetramethylsilane (TMS) as an internal standard. All the UV-vis experiments were performed in 10^{-6} M $CHCl_3$ solutions. Cyclic Voltammetry (CV) experiments were performed on Princeton Applied Research VersaSTAT 3. The transition temperatures and associated enthalpy values were determined using a differential scanning calorimeter (Perkin Elmer DSC 8000 coupled to a controlled liquid nitrogen accessory (CLN 2)) which was operated at a scanning rate of 10 °C min^{-1} both on heating and cooling. Thermogravimetric analysis (TGA) was carried out from 25 to 500 °C (at a heating rate of 10 °C min^{-1}) under nitrogen atmosphere on a Shimadzu DTG-60 instrument. Textural observations of the mesophase were performed with Nikon Eclipse LV100POL polarizing optical microscope (POM) provided with a Linkam heating stage (LTS 420). All images were captured using a Q-imaging camera. X-ray diffraction (XRD) was carried out by filling samples in glass capillaries using Cu-K$_\alpha$ (λ = 1.5418 Å) radiation from Xeuss (Model C HP100 fm) X-ray diffractometer from Xenocs equipped with GeniX 3D source operating at 50 kV and 0.6 mA in conjunction with a multilayer mirror and Pilatus 200 hybrid pixel detector from Dectris. For electroluminescence measurements compound **1.2** used as the dopants and OLED devices were fabricated by a solution-processed approach. In these OLEDs, a layer of 40 nm thick poly(3,4-ethylenedioxythiophene)polystyrene sulfonate (PEDOT:PSS) was spin-coated onto the pre-cleaned and patterned ITO substrate, which was utilized as a hole injection layer. 4,4′-bis(N-carbazolyl)-1,1′-biphenyl (CBP) was used as the host matrix, while 2,2',2"-(1,3,5-Benzinetriyl)-tris(1-phenyl-1-H-benzimidazole) (TPBi) (35 nm layer) served as the electron-transporting layer. LiF and Al were used as the composite cathode. The electroluminescence (EL) spectra were recorded using a spectra scan spectroradiometer, Photo Research PR-655. The features of the current-density and brightness versus applied voltage were simultaneously obtained by combining a Keithley 2400 and PR-655. Hole-only devices (HODs) and electron-only devices (EODs) were fabricated through a combination of spin-coating and thermal deposition of layers. In HOD, PEDOT:PSS, Di-[4-(N,N-di-p-tolyl-amino)-phenyl]cyclohexane (TAPC), and **1.2** were spin-coated on the ITO substrate, the LiF and Al were deposited by thermal evaporation. In the case of EOD, sequentially PEDOT:PSS, TPBi, and **1.2** were spin-coated on the ITO substrate. The LiF, TPBi, and Al layers were deposited by thermal evaporation.”

2) Synthesis and characterization details

Experimental Procedure:

1,3,5-tris(5-((3,4,5-tris(decyloxy)phenyl)ethynyl)thiophen-2-yl)benzene (1.1):

45 ml of dry triethylamine and 15 ml of dry DMF was taken into a 100 ml two necked RB and nitrogen gas was purged into it for 10-15 mins, compound **2**[2,3] (305.79 mg, 0.545 mmol) was dissolved into the mixture by applying slight heating. Then $Pd(PPh_3)_4$ (48.534 mg, 0.042 mmol), CuI (9.35 mg, 0.049 mmol), **3.1**[4] (1.4 g, 2.452 mmol) were added respectively. Then the temperature of the mixture was increased up to 90 ºC, left for reflux for 24 h. Upon completion, the setup was brought back to room temperature and the solvent was gotten rid of in a rotary evaporator. The mixture left was extracted using diethyl ether/water, dehydrated over anhydrous Na_2SO_4 and purification was performed using column chromatography (neutral alumina, ethyl acetate: hexane- 4.5: 95.5) and yellow colored product **1.1** was obtained (66 % yield).

^{1}H NMR (600 MHz, CD_2Cl_2, δ ppm): 7.74 (s, 3H), 7.38-7.37 (d, J = 3.8 Hz, 3H), 7.30-7.29 (d, J = 3.84 Hz, 3H), 6.75 (s, 6H), 4.00-3.94 (m, 18H), 1.83-1.78 (m, 12H), 1.74-1.68 (m, 6H), 1.50-1.45 (m, 18H), 1.37-1.27 (m, 108H), 0.90-0.86 (m, 27H).
^{13}C NMR (100 MHz, CD_2Cl_2, δ ppm): 153.68, 144.64, 139.73, 135.78, 133.48, 124.79, 124.06, 123.11, 117.53, 110.06, 95.36, 81.72, 74.04, 69.62, 32.55, 32.53, 30.35, 30.29, 30.26, 30.21, 30.02, 29.97, 29.95, 26.70, 23.30, 14.49.
IR (Neat, KBr, ν_{max}/cm^{-1}): 2954.70, 2923.98, 2871, 2853.89, 1587.40, 1574.42, 1502.33, 1466.92, 1421.49, 1386, 1354.50, 1312.24, 1233.21, 1118.17, 825.01, 750.73.
MALDI-MS: *m/z* calcd for $C_{132}H_{205}O_9S_3$ $(M+H)^+$: 2030.4746. Found: 2030.4637.

1,3,5-tris(5-((3,4,5-tris(dodecyloxy)phenyl)ethynyl)thiophen-2-yl)benzene (1.2):

Compound **1.2** was prepared by following similar procedure to **1.1**. The target material (**1.2**) was purified by using column chromatography (neutral alumina, ethyl acetate: hexane- 4.5: 95.5) to get the product as yellow semi-solid (63 % yield).

^{1}H NMR (600 MHz, CD_2Cl_2, δ ppm): 7.74 (s, 3H), 7.38-7.37 (d, *J* = 3.8 Hz, 3H), 7.30-7.29 (d, *J* = 3.8 Hz, 3H), 6.75 (s, 6H), 4.00-3.94 (m, 18H), 1.85-1.78 (m, 12H), 1.73-1.68 (m, 6H), 1.50-1.45 (m, 18H), 1.37-1.26 (m, 144H), 0.89-0.86 (m, 27H).

^{13}C NMR (100 MHz, CD_2Cl_2, δ ppm): 153.68, 144.64, 139.73, 135.79, 133.48, 124.80, 124.06, 123.14, 117.52, 110.06, 95.35, 81.71, 74.04, 69.62, 32.54, 30.35, 30.32, 30.27, 30.26, 30.01, 29.98, 29.94, 26.70, 23.30, 14.49.

IR (Neat, KBr, ν_{max}/cm^{-1}): 2954.20, 2923.43, 2871.40, 2853.21, 1587.50, 1574.90, 1502.21, 1466.80, 1421.06, 1384.30, 1354.36, 1312, 1233.32, 1119.01, 826.34, 750.84.

MALDI-MS: *m/z* calcd for $C_{150}H_{241}O_9S_3$ $(M+H)^+$: 2282.7563. Found: 2282.7468.

1,3,5-tris(5-((3,4,5-tris(tetradecyloxy)phenyl)ethynyl)thiophen-2-yl)benzene (1.3):

Compound **1.3** was prepared by following similar procedure to **1.1.** The target material (**1.3**) was purified by using column chromatography (neutral alumina, ethyl acetate: hexane- 4.5: 95.5) to get the product as pale yellow solid (70 % yield).

^{1}H NMR (600 MHz, CD_2Cl_2, δ ppm): 7.74 (s, 3H), 7.38-7.37 (d, *J* = 3.8 Hz, 3H), 7.30-7.29 (d, *J* = 3.8 Hz, 3H), 6.75 (s, 6H), 3.99-3.94 (m, 18H), 1.83-1.78 (m, 12H), 1.73-1.70 (m, 6H), 1.50-1.45 (m, 18H), 1.36-1.26 (m, 180H), 0.89-0.86 (m, 27H).

^{13}C NMR (100 MHz, CD_2Cl_2, δ ppm): 153.69, 144.64, 139.74, 135.80, 133.48, 124.80, 124.07, 123.14, 117.53, 110.07, 95.36, 81.72, 74.04, 69.62, 32.55, 30.37, 30.34, 30.31, 30.29, 30.27, 29.99, 26.71, 23.31, 14.50.

IR (Neat, KBr, ν_{max}/cm^{-1}): 2953.50, 2923.36, 2872, 2853.13, 1587.20, 1575.47, 1502.35, 1466.83, 1421.49, 1385.80, 1354.39, 1312.01, 1233.37, 1119.93, 824.21, 721.35.

MALDI-MS: *m/z* calcd for $C_{168}H_{277}O_9S_3$ $(M+H)^+$: 2535.0380. Found: 2535.0483.

3) NMR Spectra:

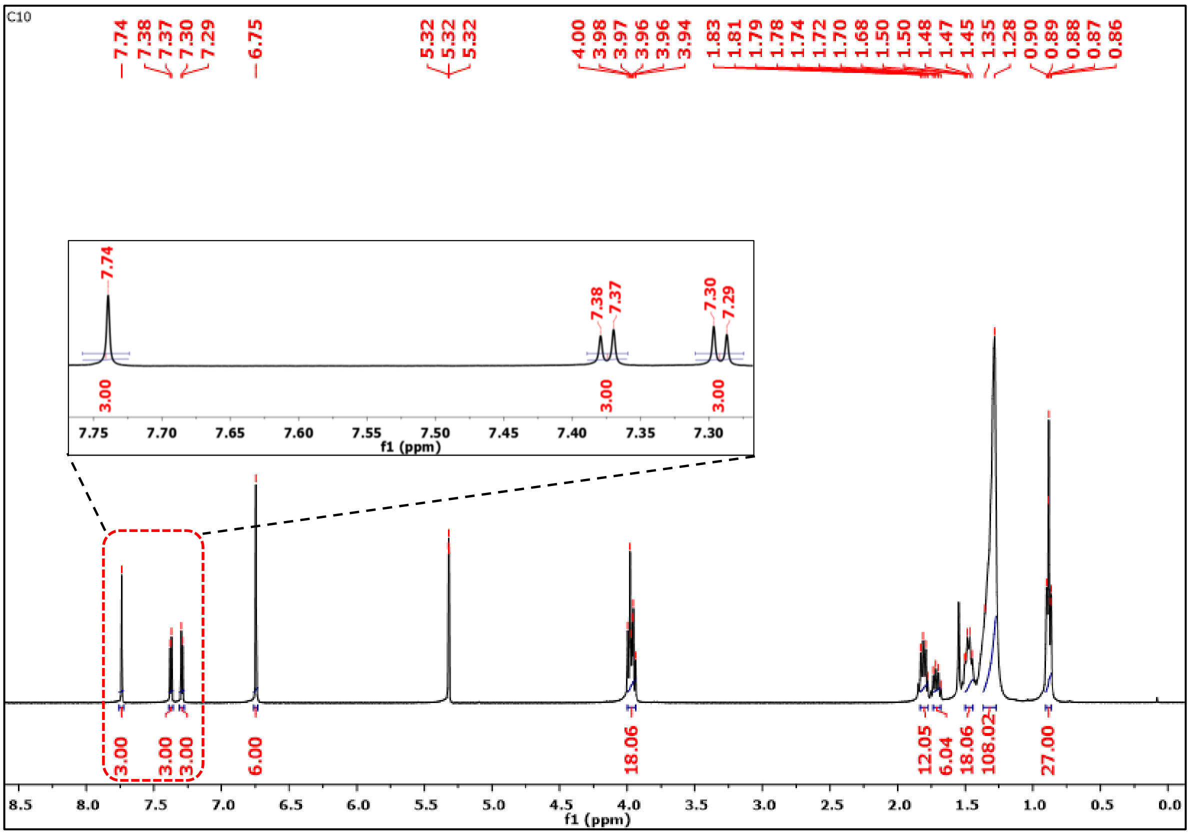

Figure S1. ^{1}H NMR of 1,3,5-tris(5-((3,4,5-tris(decyloxy)phenyl)ethynyl)thiophen-2-yl)benzene (**1.1**)

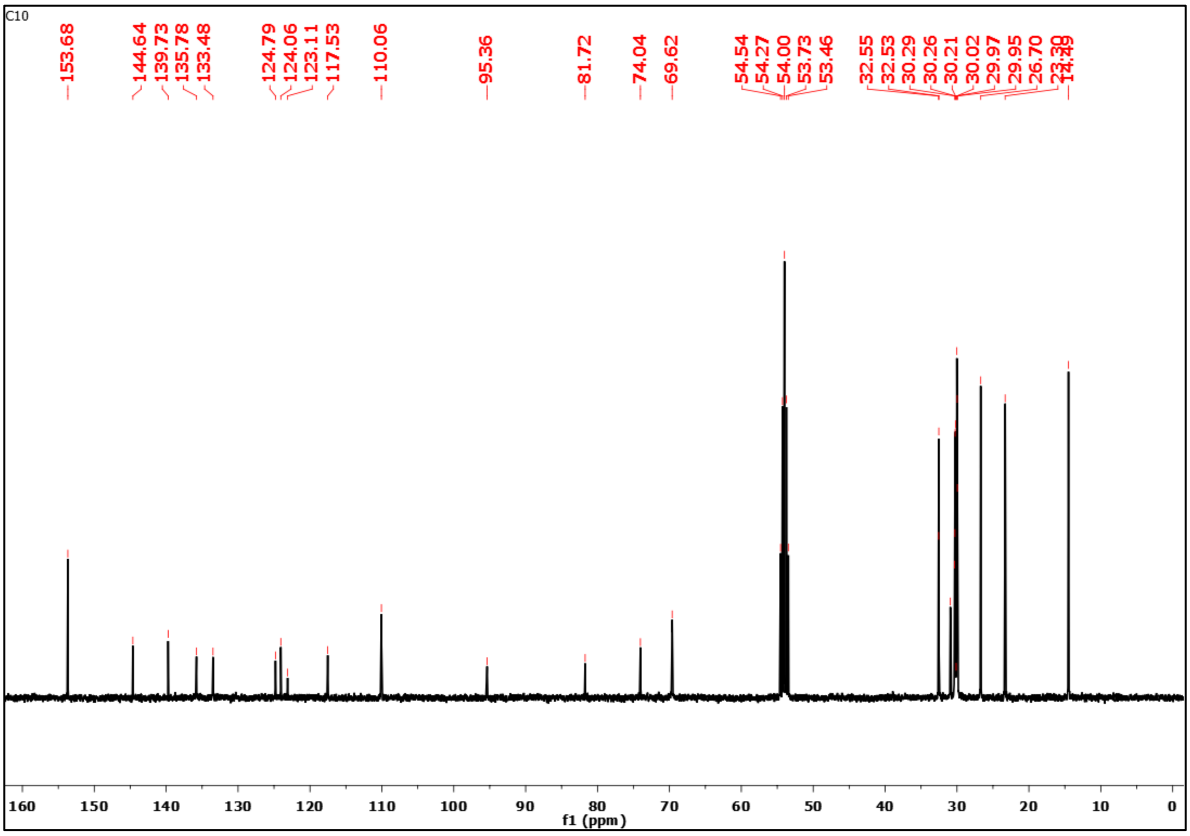

Figure S2. ^{13}C NMR of 1,3,5-tris(5-((3,4,5-tris(decyloxy)phenyl)ethynyl)thiophen-2-yl)benzene (**1.1**)

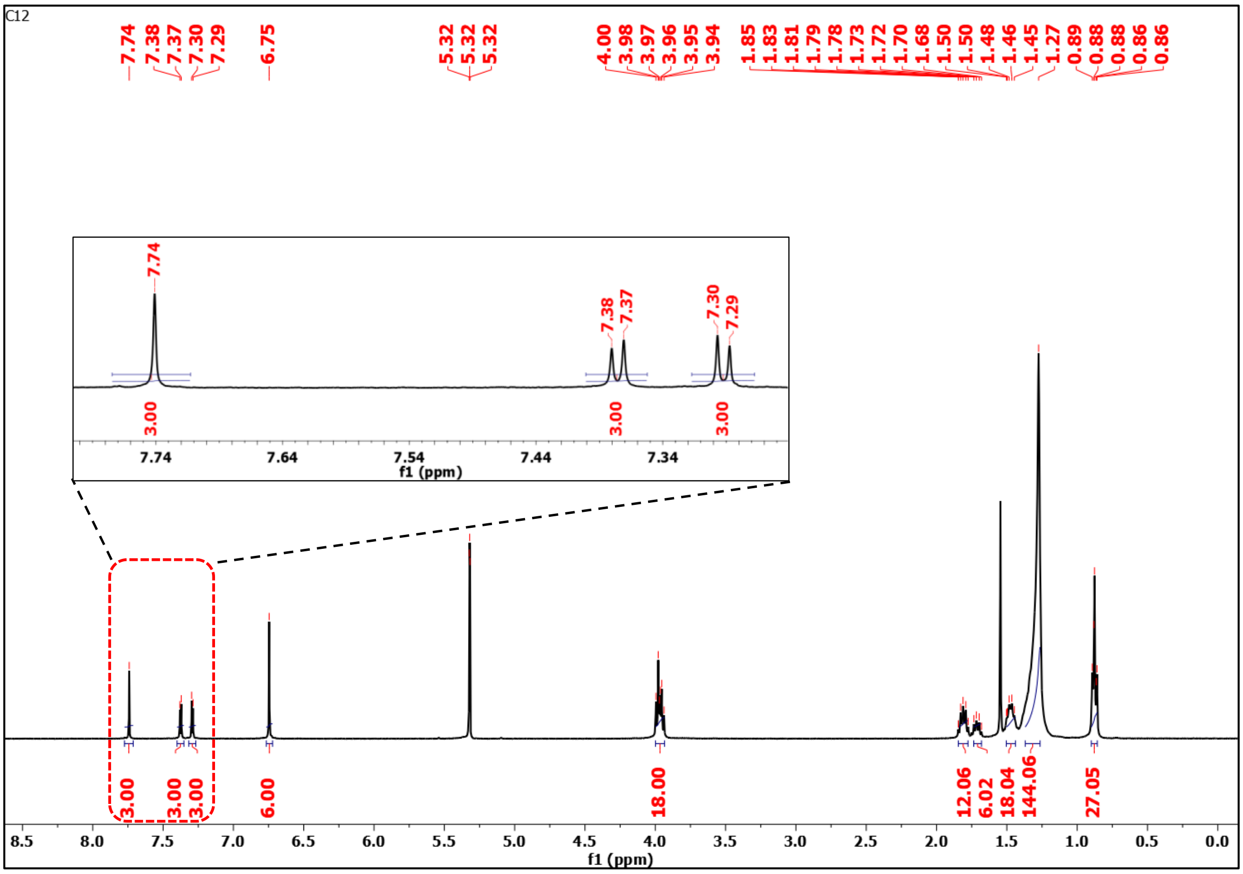

Figure S3. ^{1}H NMR of 1,3,5-tris(5-((3,4,5-tris(dodecyloxy)phenyl)ethynyl)thiophen-2-yl)benzene (**1.2**)

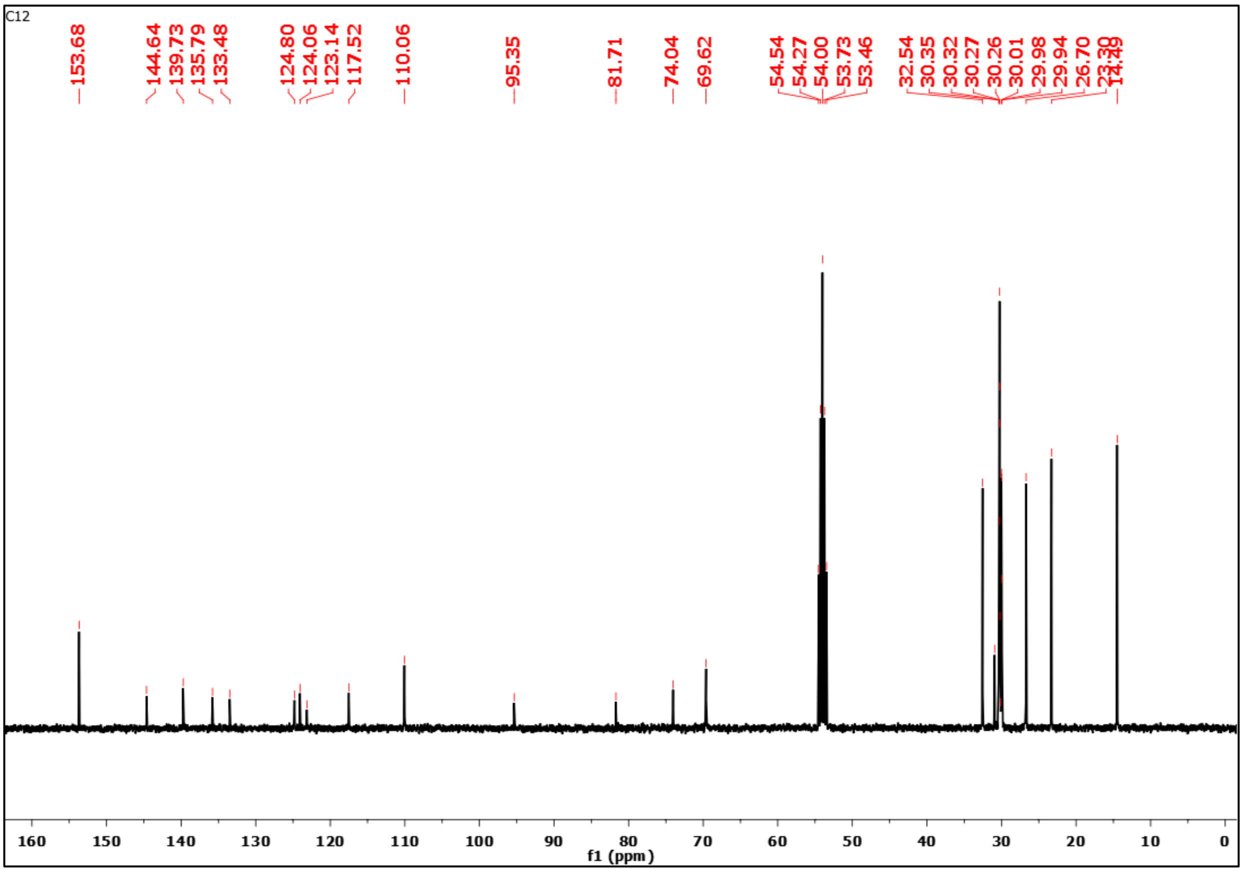

Figure S4. ^{13}C NMR of 1,3,5-tris(5-((3,4,5-tris(dodecyloxy)phenyl)ethynyl)thiophen-2-yl)benzene **(1.2)**

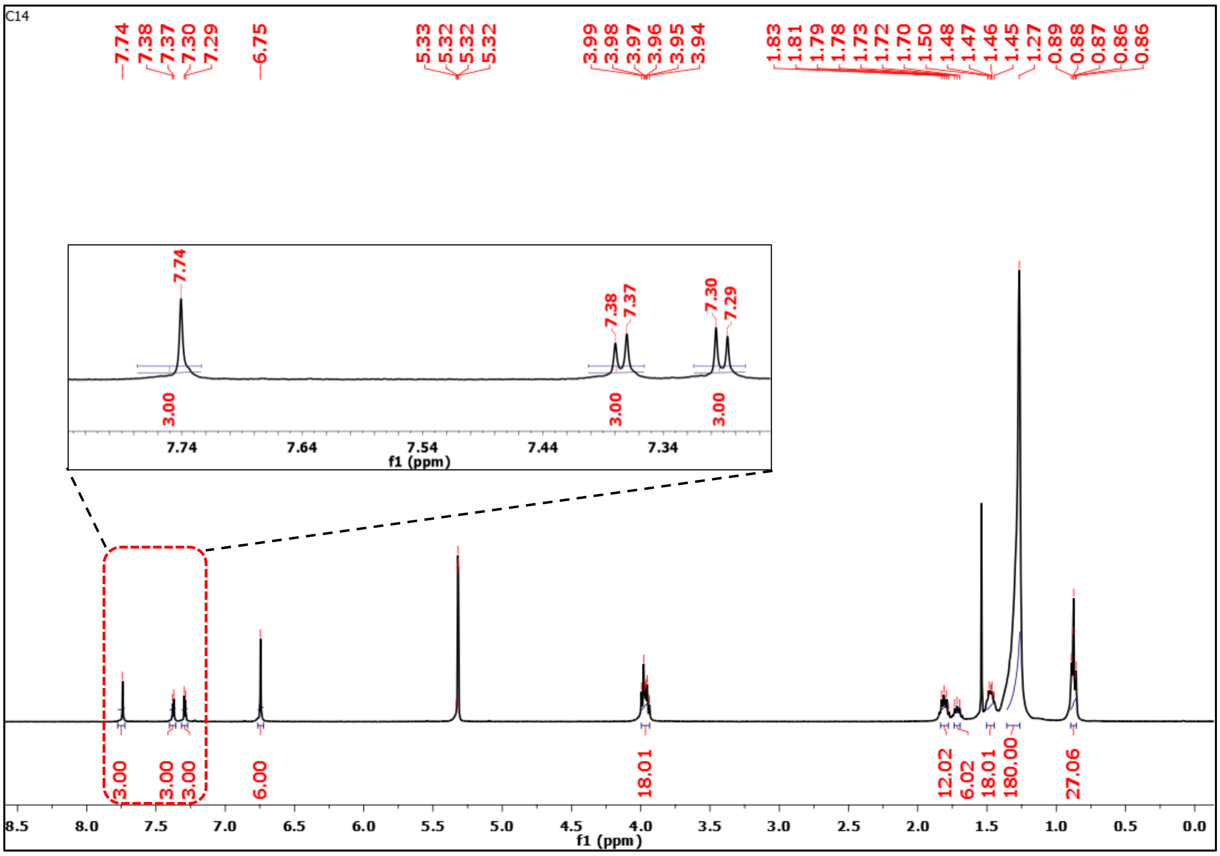

Figure S5. ^{1}H NMR of 1,3,5-tris(5-((3,4,5-tris(tetradecyloxy)phenyl)ethynyl)thiophen-2-yl)benzene (**1.3**)

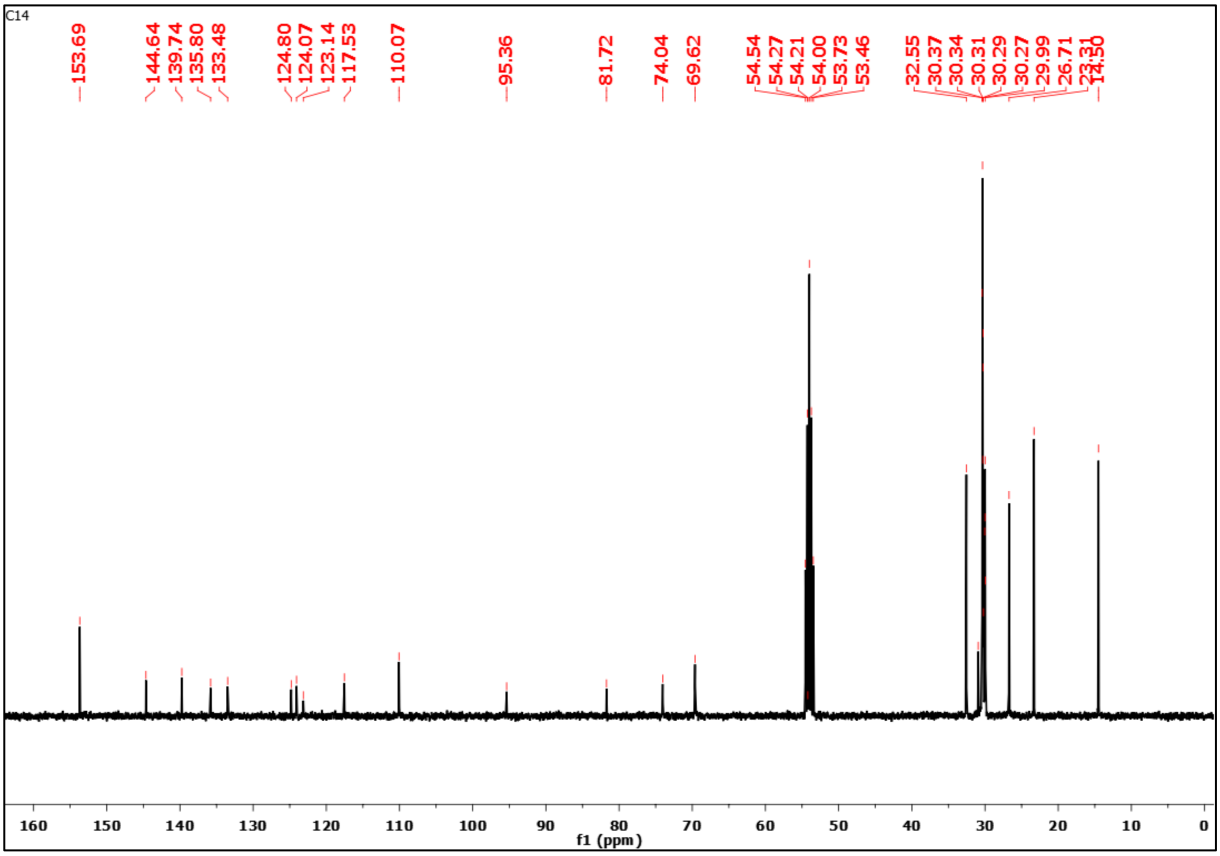

Figure S6. ^{13}C NMR of 1,3,5-tris(5-((3,4,5-tris(tetradecyloxy)phenyl)ethynyl)thiophen-2-yl)benzene (**1.3**)

4) HRMS Spectra:

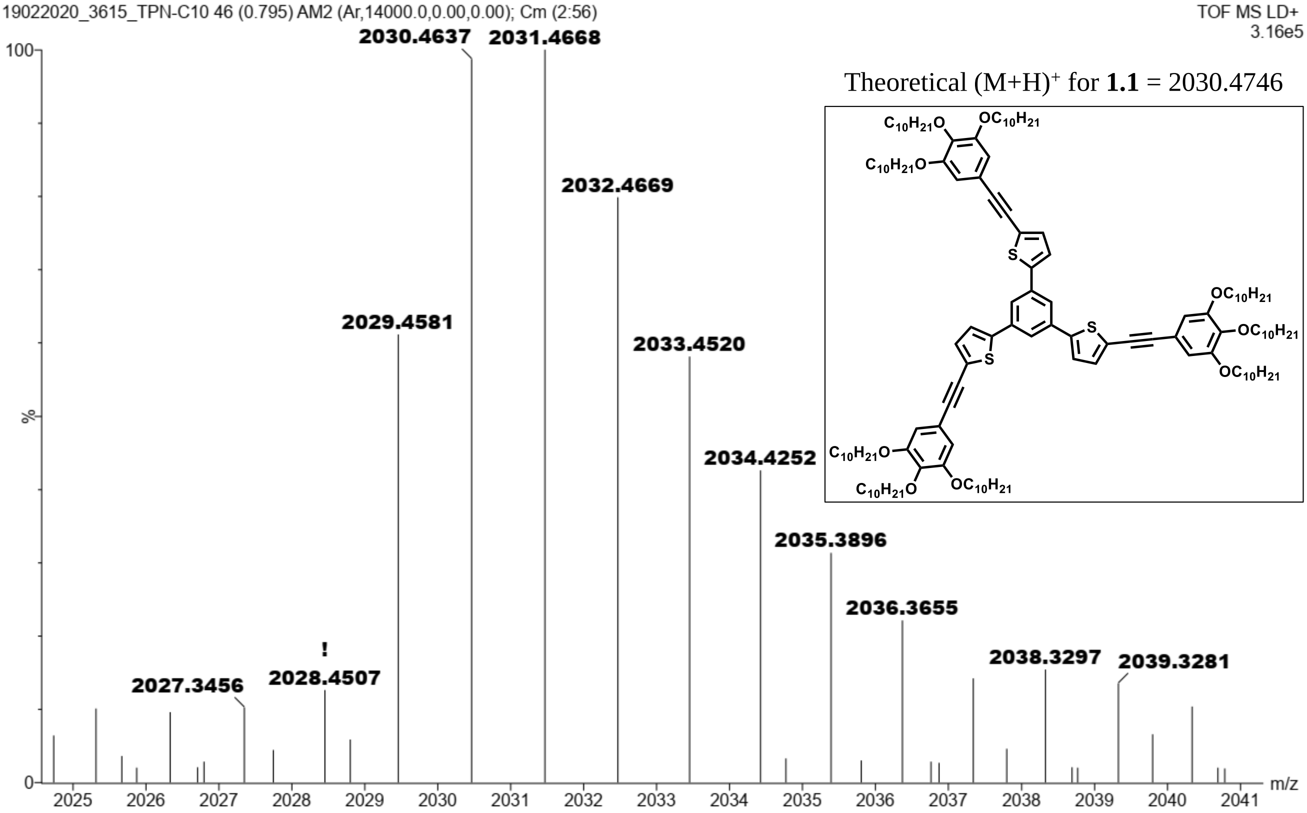

Theoretical $(M+H)^+$ for **1.1** = 2030.4746

Figure S7. HRMS spectrum of **1.1**.

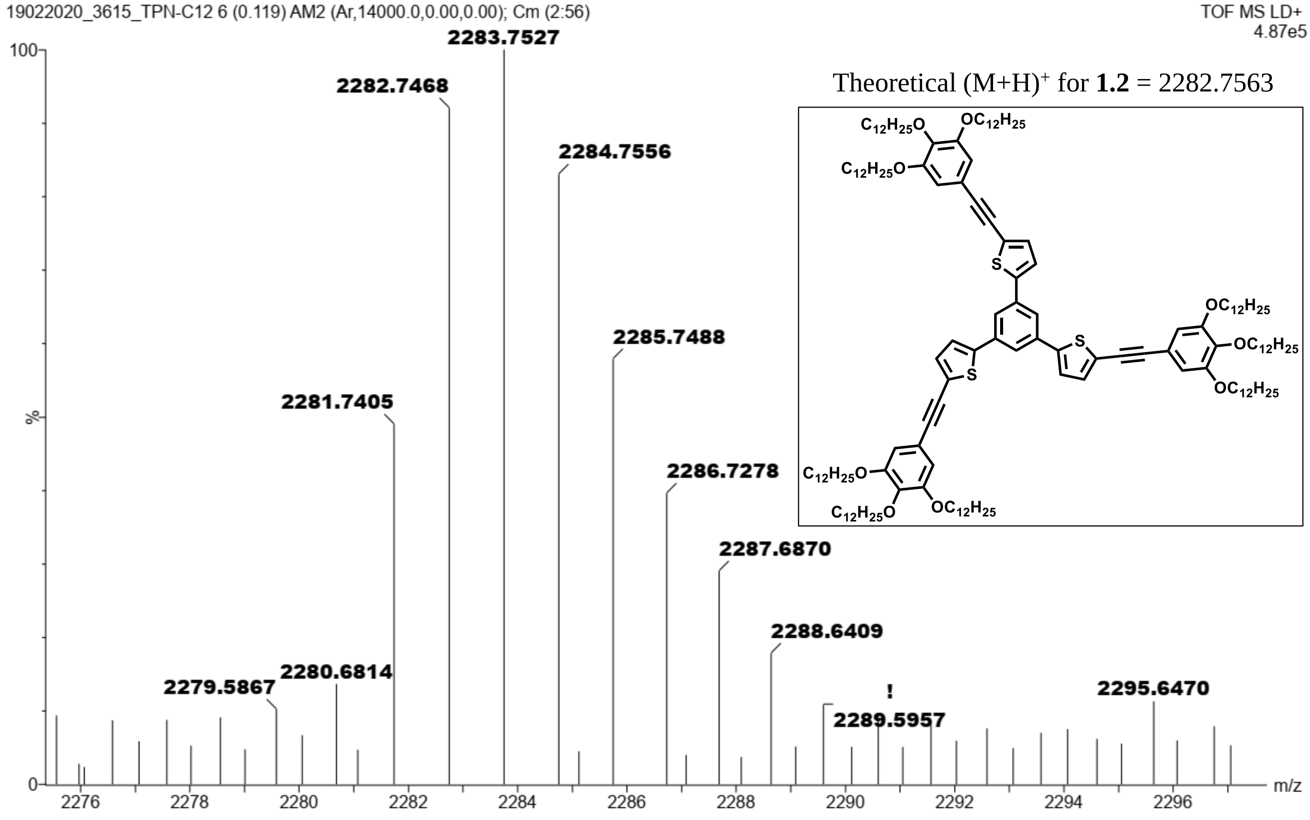

Theoretical $(M+H)^+$ for **1.2** = 2282.7563

Figure S8. HRMS spectrum of **1.2**.

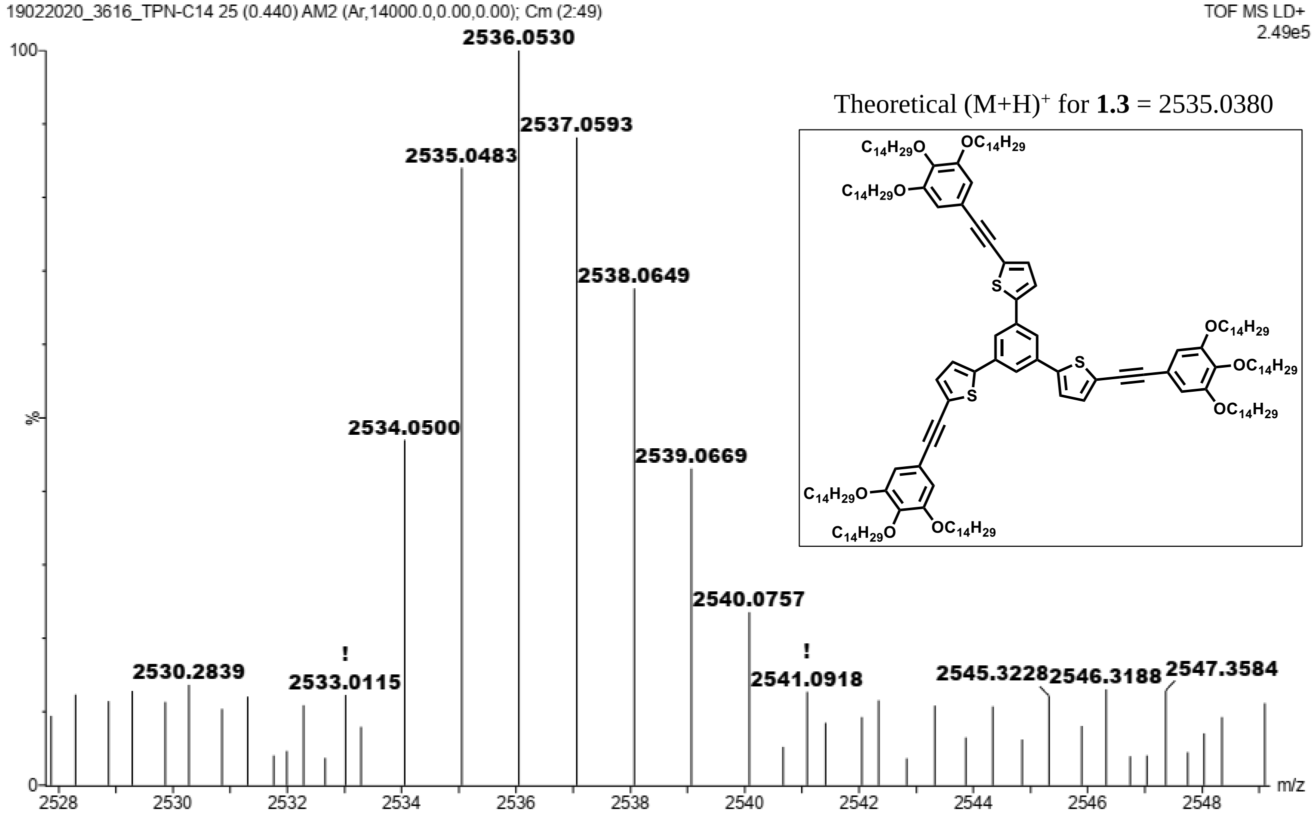

Theoretical $(M+H)^+$ for **1.3** = 2535.0380

Figure S9. HRMS spectrum of **1.3**.

5) TGA Curves:

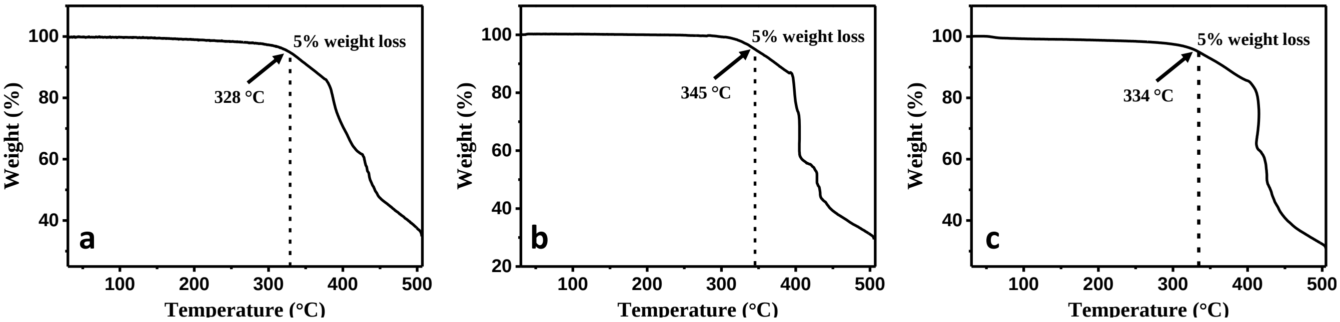

Figure S10. TGA curves of (a) **1.1**, (b) **1.2** and (b) **1.3**. The measurements were performed under a nitrogen atmosphere, with heating and cooling rates of 10 °C/min.

6) DSC Thermograms:

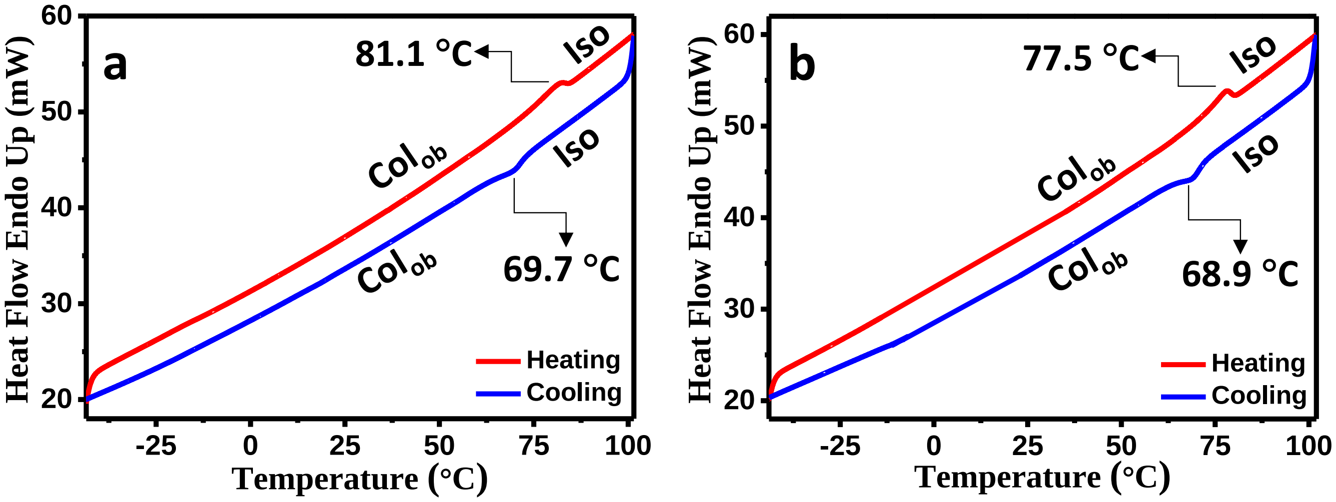

Figure S11. DSC thermograms of compound (a) **1.1** and (b) **1.3**. All the cooling and heating cycles were measured at 10 °C/min rate.

7) POM Studies:

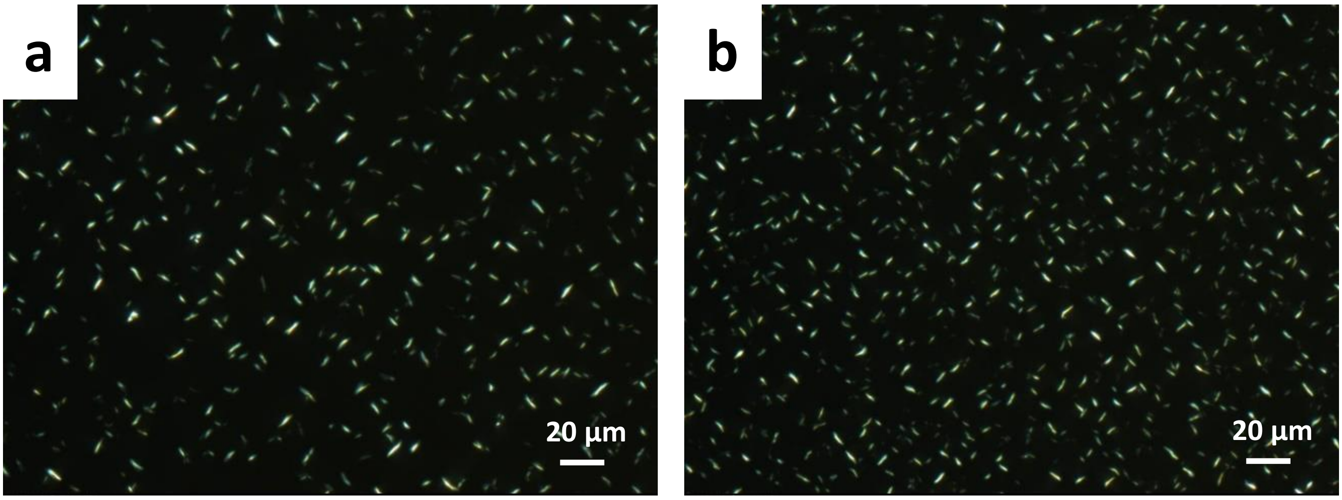

Figure S12. Polarising optical micrographs of compound (a) **1.1** at 27.2 °C and (b) **1.3** at 26.4 °C on cooling from isotropic phase.

8) X-ray Diffraction Studies:

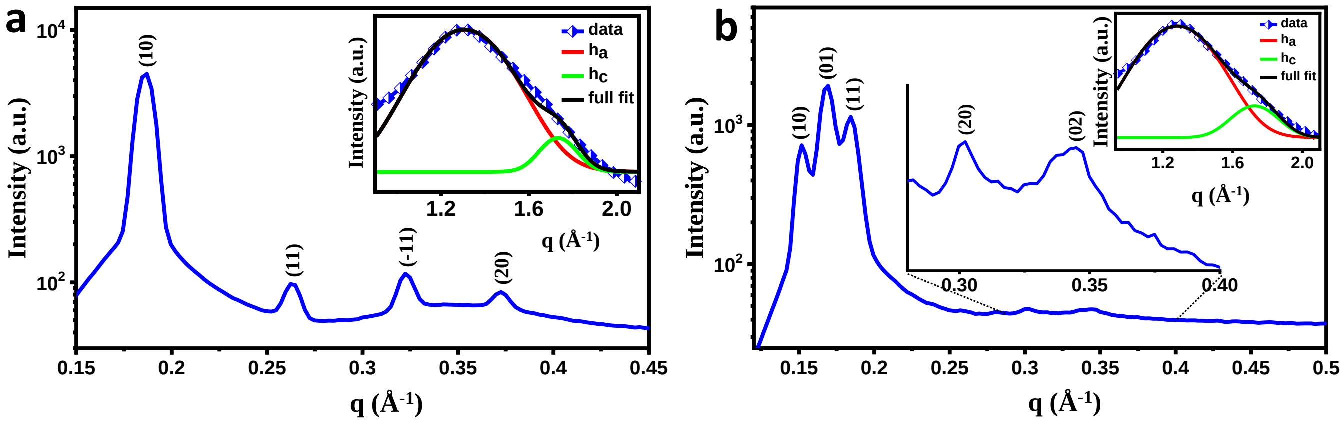

Figure S13. Small and wide angle (inset) X-ray diffraction patterns of compound (a) **1.1** and (b) **1.3** at 25 °C upon cooling.

Table S1. The indices observed and calculated *d*-spacings and planes of the diffraction peaks for compound **1.1-1.3**.

Compound	Mesophase	Lattice constants	MI[a] (*hk*)	d_{obs}[b] (Å)	d_{cal}[c] (Å)	RI[d] (hk)	M[e]	Phase Φ(hk)
1.1	Col_{ob} at 25 °C	*a* = 34.35 Å	10	33.62	33.629	100.00	2	0
		b = 28.25 Å	11	23.89	23.89	2.16	2	0
		α = 78.19°	-11	19.49	19.49	2.60	2	0
			20	16.87	16.81	1.87	2	π
			h_a	4.84				
			h_c	3.75				
1.2	Col_{ob} at 25 °C	*a* = 36.34 Å	10	35.54	35.54	100.00	2	0
		b = 29.60 Å	11	25.17	25.17	2.13	2	0
		α = 77.93°	-11	20.45	20.45	1.79	2	0
			20	17.75	17.77	1.44	2	π
			h_a	4.92				
			h_c	3.80				
1.3	Col_{ob} at 25 °C	*a* = 44.12 Å	10	41.42	41.42	37.30	2	0
		b = 39.53 Å	01	37.11	37.11	100.00	2	0
		α = 69.84°	11	34.09	34.09	96.14	2	0
			20	20.79	20.71	2.45	2	π
			02	18.44	18.55	2.61	2	π
			h_a	4.88				
			h_c	3.73				

[a] MI: Miller indices. [b]d_{obs} :experimental *d*-spacing. [c]d_{cal} : calculated *d*-spacing by using the relation $\frac{1}{{d_{cal}}^2} = \frac{1}{(\mathrm{Sin}\alpha)^2}\left[\frac{h^2}{a^2} + \frac{k^2}{b^2} - \frac{2\,h\,k\,\mathrm{Cos}\alpha}{ab}\right]$ where *a*, *b* and angle α are the lattice parameters of the oblique lattice. [d] RI: Relative Intensity. [e]M: Multiplicity.

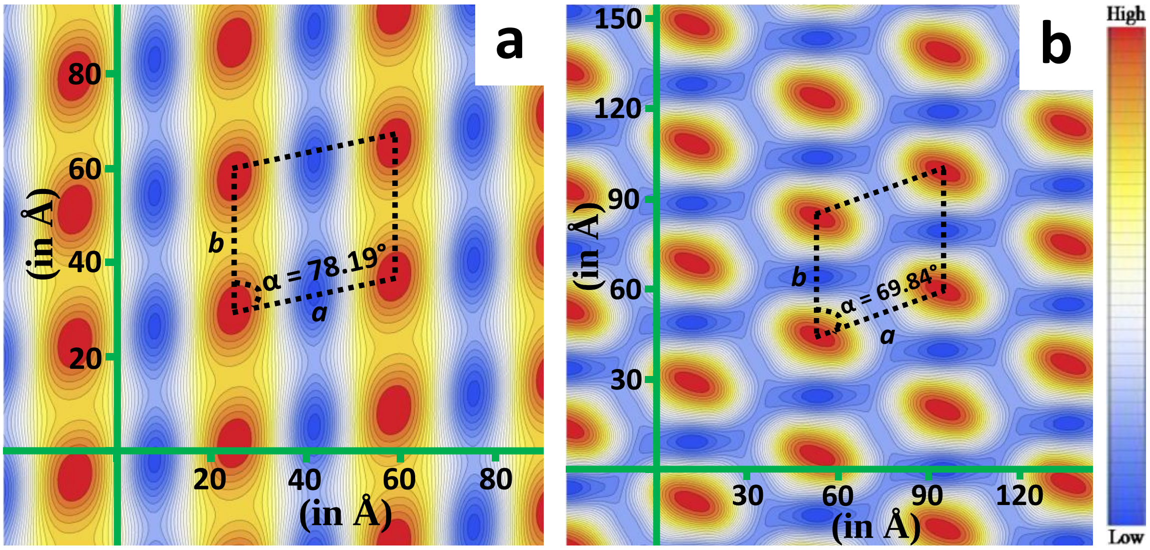

Figure S14. Electron density map of compound (a) **1.1** and (b) **1.3** in Col$_{ob}$ mesophase.

9) Photophysical Studies:

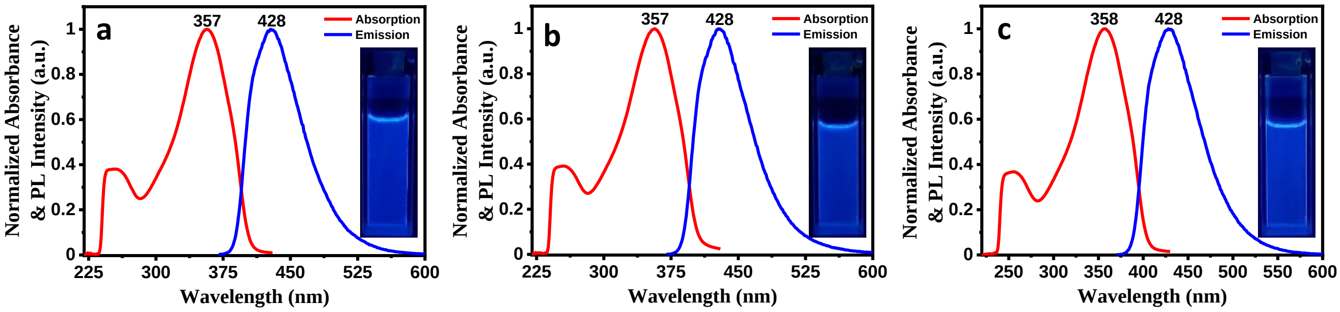

Figure S15. UV-vis absorption and PL emission spectra of (a) **1.1**, (b) **1.2** and (c) **1.3** in chloroform solvent of 10^{-6} M concentration. Insets show the blue emission under 365 nm UV light.

10) Electrochemical Studies:

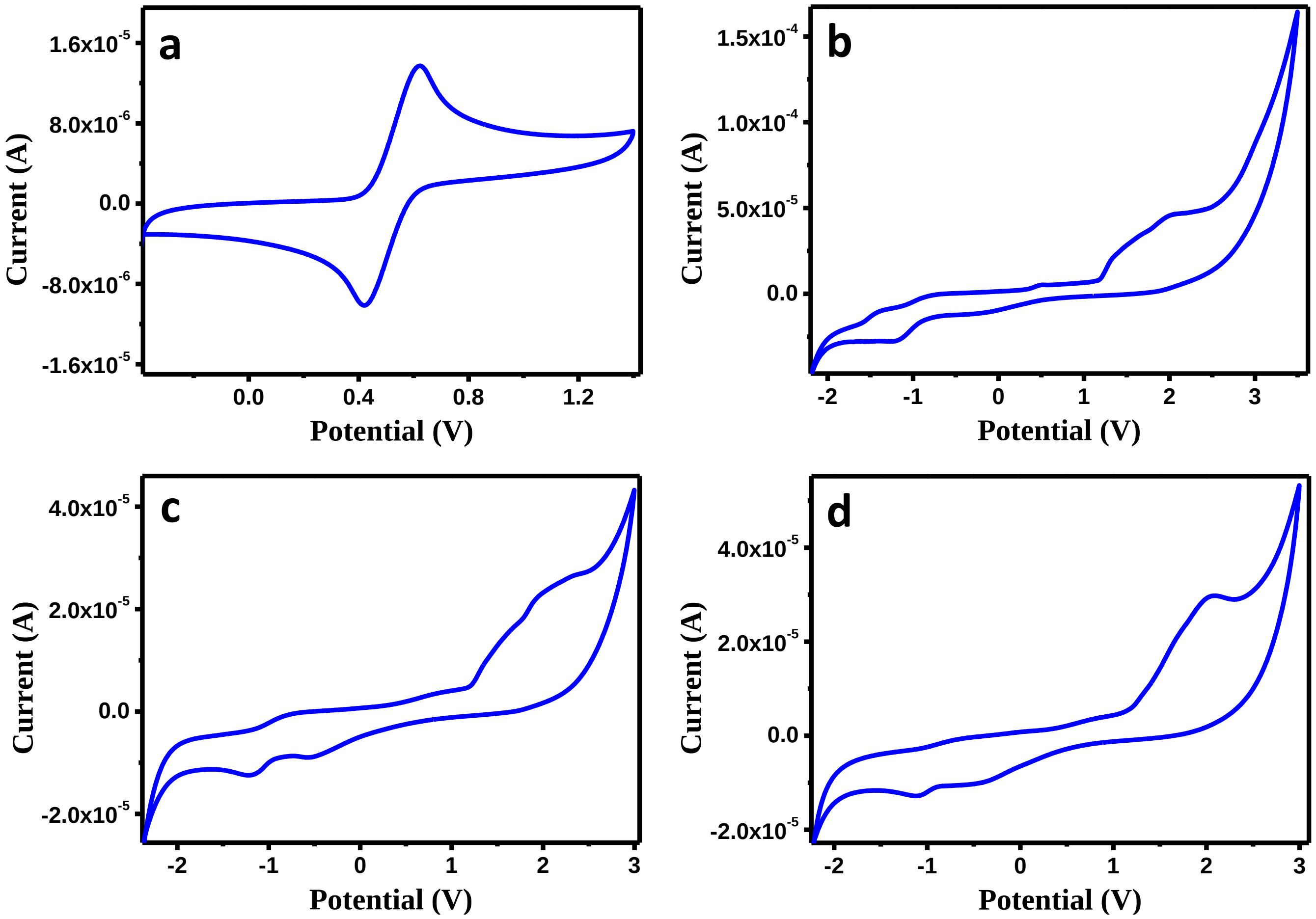

Figure S16. Cyclic voltammogram of (a) ferrocene, compound (b) **1.1**, (c) **1.2** and (d) **1.3** in HPLC dichloromethane solution of tetrabutylammonium perchlorate (TBAP (0.1 M)) at a scan rate of 50 mVs^{-1} (Experimental conditions: Ag/AgNO$_3$ as reference electrode, platinum wire as counter electrode, glassy carbon as working electrode, TBAP (0.1 M) as supporting electrolyte, room temperature).

Table S2. Electrochemical properties of compounds **1.1-1.3**.

Compound	E_{HOMO} [a] (eV)	E_{LUMO} [b] (eV)	$\Delta E_{g,CV}$ [c] (eV)
1.1	-5.48	-3.44	2.04
1.2	-5.49	-3.42	2.07
1.3	-5.47	-3.43	2.04

[a] Estimated from the formula $E_{HOMO} = -(4.8 - E_{1/2,Fc,Fc^+} + E_{oxd,onset})$ eV. [b] Estimated from the onset reduction peak values using $E_{LUMO} = -(4.8 - E_{1/2,Fc,Fc^+} + E_{red,onset})$ eV. [c] Estimated from the formula $\Delta E_{g,CV} = E_{LUMO} - E_{HOMO}$.

11) Computational Studies:

To understand the electronic properties and frontier molecular orbital energy level of compound **1.2**, theoretical calculations were carried out with the Gaussian 09 suite of packages.[5] A full optimization was carried out using the hybrid functional, Becke's three parameter exchange and the LYP Correlation Functional (B3LYP)[6] at a split valence basis set 6-31G(d,p). The optimized geometry and frontier molecular orbitals for the **1.2** are shown in Figure S17.

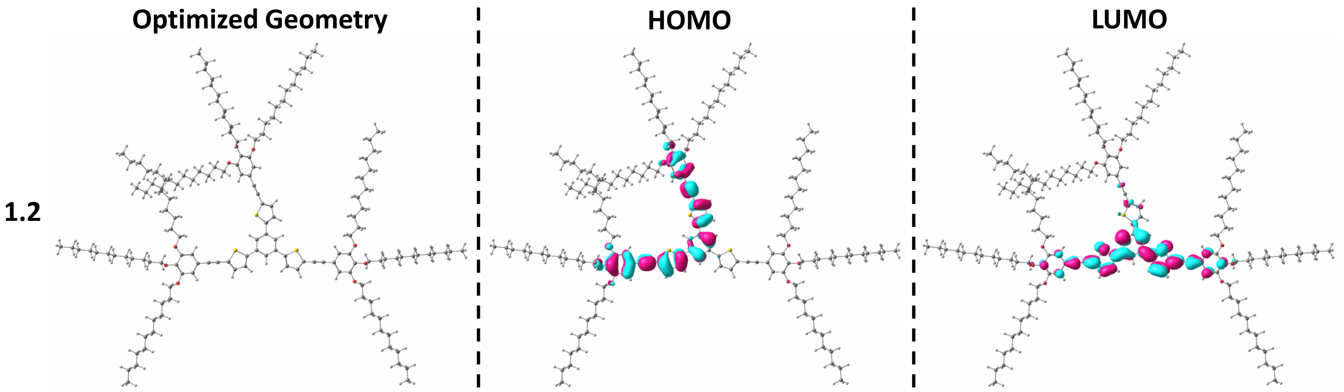

Figure S17. Optimized geometry and electronic distribution of frontier molecular orbitals (HOMO and LUMO) of compound **1.2**.

12) OLED Device Fabrication data:

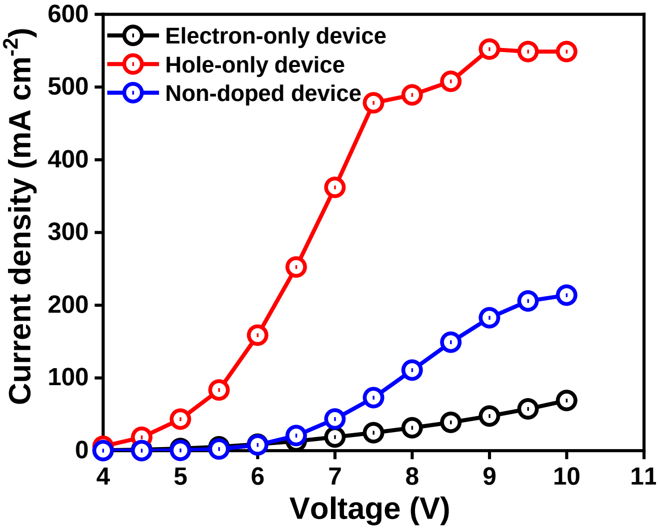

Figure S18. Current density-voltage curves of hole-only devices (HOD: ITO (125 nm)/ PEDOT:PSS (40 nm)/ TAPC (35 nm)/ **1.2** (22 nm)/ TAPC (35 nm)/ LiF (1.0 nm)/ Al (150 nm)), electron-only devices (EOD: ITO (125 nm)/ PEDOT:PSS (40 nm)/ TPBi (35 nm)/ **1.2** (22 nm)/ TPBi (35 nm)/ LiF (1.0 nm)/ Al (150 nm)) and non-doped device (ITO (125 nm)/ PEDOT:PSS (40 nm)/ **1.2** (22 nm)/ TPBi (35 nm)/ LiF (1.0 nm)/ Al (150 nm).

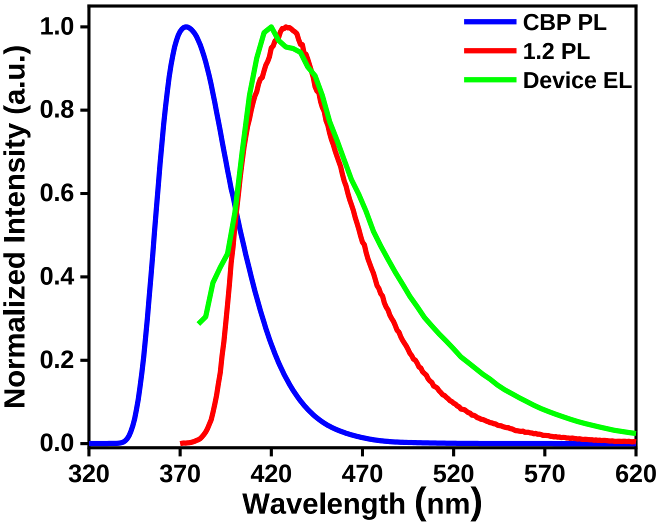

Figure S19. Photoluminescence emission spectra of CBP and **1.2** compared with the CBP:**1.2** based device electroluminescent spectra.

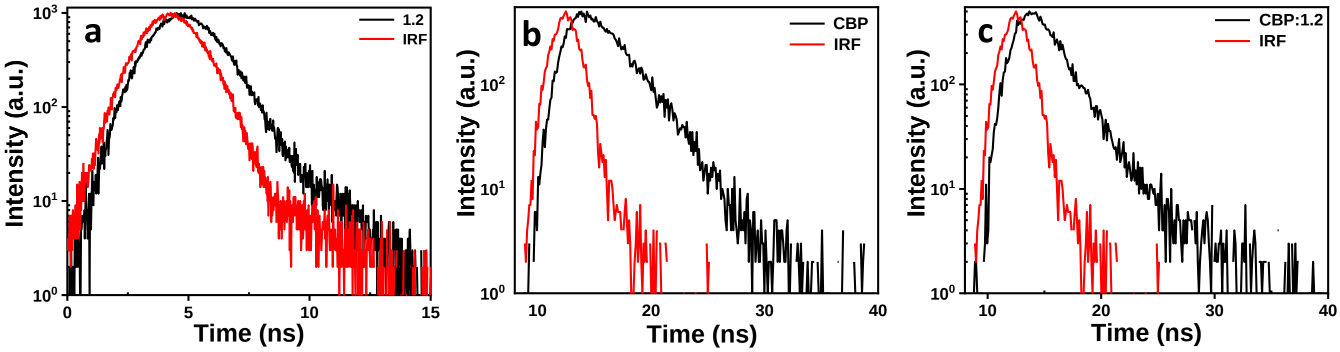

Figure S20. Transient PL decay of (a) **1.2**, (b) CBP, and (c) CBP:**1.2** system.

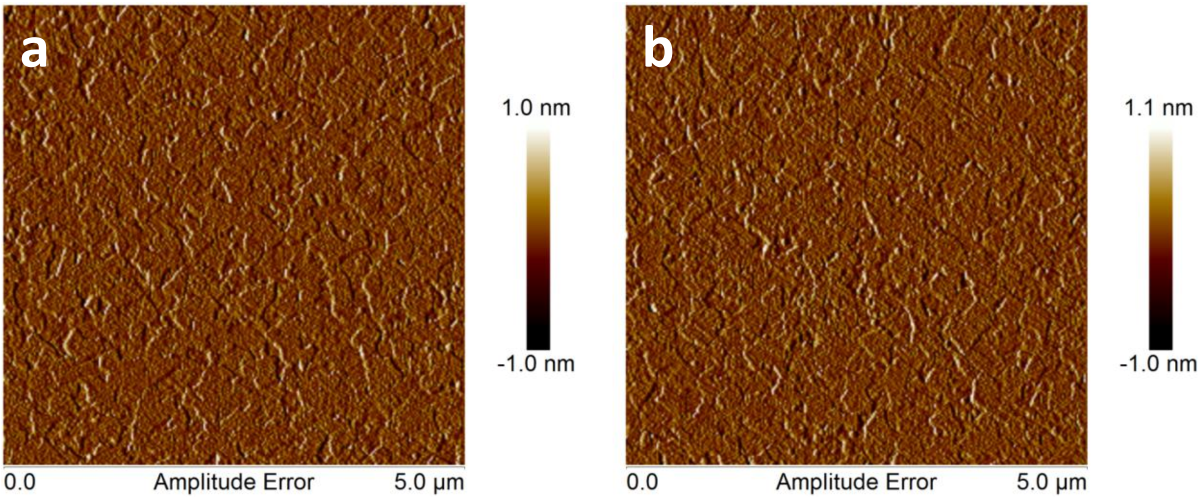

Figure S21. AFM images of the spin-coated films of (a) CBP:**1.2** (3.0 wt%) and (a) **1.2**.

Table S3. Effect of **1.2** doping concentration on the turn-on voltage (V_{on}), power efficiency (PE), current efficiency (CE), external quantum efficiency (EQE), CIE coordinates, and maximum luminance of solution-processed deep-blue OLED devices with the CBP host.

Dopant concentration (wt%)	Turn-on voltage[a] (V_{on})	PE_{max}/ CE_{max}/ EQE_{max}[b] (lm W^{-1}/ cd A^{-1}/ %)	PE_{100}/ CE_{100}/ EQE_{100}[c] (lm W^{-1}/ cd A^{-1}/ %)	CIE_{xy} Coordinates[d]	Maximum Luminance (cd m^{-2})
1.0	5.1	1.2/ 2.2/ 4.4	0.6/ 1.2/ 2.9	(0.16, 0.06)	1360
3.0	5.5	1.2/ 2.3/ 4.7	0.5/ 1.1/ 2.9	(0.16, 0.05)	1191
5.0	5.1	0.6/ 1.1/ 2.3	0.5/ 1.0/ 2.3	(0.16, 0.06)	1039
100	5.4	- / - / -	- / - / -	-	69

[a]Turn-on voltage (V_{on}) (luminance > 1 cd m^{-2}), [b] Maximum Power efficiency (PE_{max}), current efficiency (CE_{max}), and external quantum efficiency (EQE_{max}) of the device, [c] Power efficiency (PE), current efficiency (CE), and EQE at 100 cd m^{-2} and [d]CIE coordinates at 100 cd m^{-2}.

13) References:

1. J. De, S. P. Gupta, S. S. Swayamprabha, D. K. Dubey, I. Bala, I. Sarkar, G. Dey, J. H. Jou, S. Ghosh and S. K. Pal, *J. Phys. Chem. C*, 2018, **122**, 23659.
2. W. J. Mitchell, N. Kopidakis, G. Rumbles, D. S. Ginley and S. E. Shaheen, *J. Mater. Chem.*, 2005, **15**, 4518.
3. B. M. Schulze, D. L. Watkins, J. Zhang, I. Ghiviriga and R. K. Castellano, *Org. Biomol. Chem.*, 2014, **12**, 7932.
4. I. Bala, J. De, S. P. Gupta, H. Singh, U. K. Pandey and S. K. Pal, *Chem. Commun.*, 2020, **56**, 5629.
5. M. J. Frisch, *et* al. Gaussian 09 (Revision D.01) Gaussian, Inc., Wallingford CT, 2009**.**
6. A. D. Becke, *J. Chem. Phys.*, 1993, **98**, 5648.